ACS APPLIED POLYMER MATERIALS

pubs.acs.org/acsapm

Article

Solution Structure and Counterion Condensation of Carboxymethyl Cellulose in Organic Solvents

Published as part of ACS Applied Polymer Materials special issue "Polyelectrolytes: Bridging Electrostatics, Interfaces, and Materials Science".

Anish Gulati, Lingzi Meng, Can Hou, Takaichi Watanabe, and Carlos G. Lopez*

Cite This: ACS Appl. Polym. Mater. 2026, 8, 8183–8197

Read Online

ACCESS | Metrics & More | Article Recommendations | Supporting Information

ABSTRACT: We report scattering (SANS and SAXS) and electrical conductivity data for aqueous and organic solutions of carboxymethyl cellulose with tetrabutylammonium counterions. For SANS in deuterated solvents, the contrast is heavily dominated by the hydrogen-rich counterions, while for SAXS the polymer backbone has a more significant contribution to the scattering signal. The correlation length calculated from the SAXS measurements follows a scaling law of $\xi \propto c^{-1/2}$, while that measured by SANS displays a weaker exponent at higher concentrations for solvents of high dielectric constants. These results indicate a decoupling in the characteristic length scales of fluctuations of the polymer backbone and counterions at high polyelectrolyte concentrations. The stretching parameter calculated from the correlation length indicates a highly stretched local conformation for TBACMC in water and several high dielectric constant solvents, consistent with the semiflexible nature of the cellulose backbone. In solvents of lower dielectric permittivity, the chains display a higher degree of local coiling. Combining electrical conductivity and scattering data, we find that the fraction of monomers bearing a dissociated charge is nearly independent of concentration and approximately proportional to the reciprocal of the Bjerrum length of the solvent, as expected by the Oosawa-Manning model.

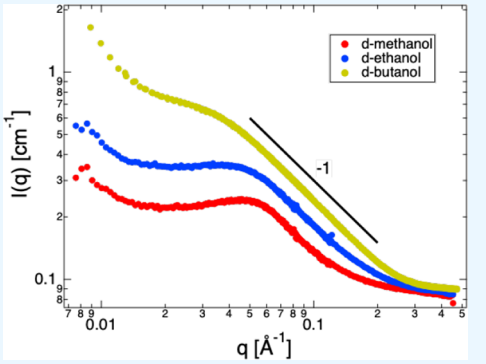

KEYWORDS: *polyelectrolyte, scattering, conductivity, cellulose, condensation*

1. INTRODUCTION

Polyelectrolytes are a class of ion-containing polymers in which all of the ionic groups bear charges of the same sign.[1−4] The presence of charged groups on the polymer backbone enhances their solubility in polar solvents and allows them to form complexes with oppositely charged species.[5−8] By independently tuning the polymer backbone and counterions, orthogonal functionality can be introduced, allowing specific properties such as responsiveness to environmental factors (e.g., temperature, pH, and ionic strength).[9,10]

Water is, without a doubt, the most important solvent for charged polymers due to its relevance to living organisms, where polyelectrolytes play a role in many physiological processes.[11−15] Because of this, the vast majority of the experimental polyelectrolyte literature focuses on the properties of aqueous solutions.[16,17] The lack of comprehensive studies on polyelectrolytes in nonaqueous media results in two limitations in our fundamental understanding of polyelectrolyte solutions. First, the role of solvent permittivity on the properties of polyelectrolytes[18−20] has not been systematically studied, with most work being carried out at a fixed dielectric constant of $\epsilon \simeq 78$. Second, the influence of polymer and counterion−solvent interactions[21−24] on the thermodynamics, structure, and rheology of polyelectrolytes remains largely unexplored.[17] Understanding how dielectric constant and other solvent properties affect charged polymers is relevant for applications such as batteries[25] and membranes.[26−30]

The dielectric constant of the solvent sets the strength of electrostatic interactions between charges in solution. In the absence of electrostatic screening, the Coulomb energy (U_C) for a pair of oppositely charged ions a distance r $U_C/k_BT = -l_B/r$, where k_B is Boltzmann's constant, T is the absolute temperature, and l_B is the Bjerrum length. The Bjerrum length is the distance at which the electrostatic and thermal energies of a pair of monovalent ions in solution are equal:

$$l_B = \frac{e^2}{4\pi k_B T \epsilon_0 \epsilon}$$

Received: February 4, 2026
Revised: May 20, 2026
Accepted: May 21, 2026
Published: May 30, 2026

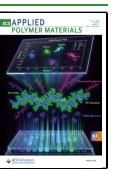

where e is the electrostatic unit of charge, ϵ is the dielectric constant or relative permittivity of the solvent, and ϵ_0 is the vacuum permittivity.

The coupling parameter (u) is defined as the ratio between the Bjerrum length and the distance between ionic groups on the backbone. The distance between charges is given by the ratio of the length of a chemical monomer (b) and the number of charges per monomer unit (n),

$$u = nl_B/b$$

The theory of counterion condensation[31−33] predicts that when the coupling parameter exceeds unity, counterions condense onto the polymer backbone, neutralizing the ionic groups so as to bring the effective charge density to a value of one charge per Bjerrum length. The effective charge density of the backbone (μ_{eff}) is

$$\mu_{eff} = \begin{cases} e \cdot n/b & \text{if } u < 1 \\ e/l_B & \text{if } u > 1 \end{cases} \quad (1)$$

Counterion condensation is essential to understanding polyelectrolyte solutions because virtually all polyelectrolyte properties, from osmotic pressure or charge transport to the rheological properties of solutions, are dependent on the effective charge of the chains.[17,34,35]

While Oosawa and Manning derived their theories for single chains (i.e., solutions in the infinite dilution limit), results by Wandrey et al.[36,37] show that the Oosawa-Manning (OM) threshold for salt-free solutions applies only in the semidilute regime. Below the overlap point, the fraction of free counterions increases upon dilution, in agreement with the two-phase model of Liao et al.[38]

Nyquist et al.[39] find broad agreement with Manning's theory but predict a less sharp dependence of the fraction of condensed counterions on the bare charge density. Theoretical work by Muthukumar and coworkers[40−42] expects strong deviations from the Oosawa-Manning model for flexible chains. In brief, their theory predicts that because counterion adsorption influences chain conformation, a self-consistent calculation of the free energy of the polyelectrolyte (chain and counterions) is necessary to estimate the fraction of free counterions.[43] These works also predict that the dielectric mismatch, which is proportional to the relative difference between the dielectric constant in the bulk and around the polymer chains, can significantly alter counterion adsorption profiles. When plotting f as a function of Bjerrum length at constant dielectric mismatch, Muthukumar and coworkers observe much sharper dependencies than the Oosawa-Manning model. A difficulty that arises in checking these predictions is the lack of experimental methods to quantify the dielectric mismatch.

Equation 1 can be experimentally tested in two ways: first, by altering the chemical composition of the backbone, the value of n can be changed. Dou and Colby[44] quaternized poly(2-vinylpyridine) to different degrees and used electrical conductivity measurements to evaluate the effective charge density of the chain in semidilute ethylene glycol solutions.[44] Their results agree with several aspects of the OM model: the $\mu_{eff} \propto n$ and $\mu_{eff} \propto n^0$ at low and high charge density are approximately observed, and the crossover occurs at u ≈ 1, but the transition between these two regimes was broader than expected by eq 1. The effective charge density in the high charge density region is close to e/l_B as expected by eq 1. Kowblansky and Zema[45] studied the activity of counterions in copolymers of acrylic acid and acrylamide with varying charge density, finding reasonable agreement with Manning's theory.

The second approach to test eq 1 is to keep the chemical composition of the polymer constant (i.e., constant n) and vary the dielectric constant of the solvent. Here, fewer studies, mostly relying on indirect measurements of the effective charge fraction, have been performed: in one study, Beer et al. fit a Flory theory to radius of gyration vs added salt concentration data for polyvinylpyridine derivatives, which allowed them to extract the effective charge fraction and intrinsic excluded volume.[18] This yielded an unusual dependence of $\mu_{eff} \simeq (\epsilon - 16)^{1/2}$, which does not agree with Oosawa-Manning. In another study, Lopez et al.[17] used the scaling theory[46] to calculate f from overlap concentration data of two poly(ionic liquids).[19,47] A stronger-than-anticipated dependence of $\mu_{eff} \propto \epsilon^{1.6}$ was found. This relationship was obtained on the assumption that all solvents considered act as θ solvents for the backbone, which could not be verified.

Studying nonaqueous solvents can yield insight into the nature of electrostatic forces in polyelectrolyte solutions. This is challenging because of the limited solubility of most polyelectrolytes in nonaqueous media.[48,49] One way of overcoming this difficulty is to increase the affinity of the counterions for the solvent.[50] This approach was pioneered by Ono and coworkers[51−54] and Chen et al.[55] to develop cross-linked polyelectrolyte networks with high absorption capacity for nonpolar solvents. More recently, the tetra-alkylammonium salts of polystyrenesulfonate and carboxymethyl cellulose were found to be soluble in many protic, polar solvents.[20,56,57]

1.1. Prior Work on CMC Solutions

Carboxymethyl cellulose is a semiflexible, weak, anionic ether of cellulose made by reacting chloroacetic acid with activated cellulose.[58−60] The average number of carboxymethyl groups (out of three hydroxyl groups in the glucose unit) per monomer is known as the degree of substitution, or DS. Commercially, carboxymethyl cellulose is used as the sodium salt (NaCMC) with DS $\gtrsim$ 0.7, as required for solubility in water. Higher substitution degrees are used to ensure a more regular substitution pattern, which prevents gelation of CMC at high polymer concentrations.[61−63] The many applications of CMC in the food, pharmaceutical, paper, and oil industries, as well as potential applications in new technologies[64−66] have led to extensive investigations into its physical properties.

1.1.1. Counterion Condensation. The first systematic studies on the effective charge fraction of NaCMC used potentiometry and osmotic pressure to determine the activity and osmotic coefficients of CMC solutions with various monovalent and divalent counterions.[67−73] The effective charge of the chain was found to be inversely proportional to the counterion valence, as predicted by the Oosawa-Manning model. For a given counterion valence, the counterion type has a large influence on the degree of ion-pair formation[74−79] but not on the fraction of free counterions.[67,71,80] The effective charge fractions obtained from these studies were reviewed recently and found to qualitatively agree with Oosawa-Manning.[80]

Cametti and coworkers[81,82] studied the dielectric response of two NaCMC polymers in aqueous solutions. The DC conductivity was used to estimate the fraction of free counterions as a function of polymer concentration. For sufficiently dilute solutions, all of the counterions were found to be dissociated. Solutions above the overlap concentration

https://doi.org/10.1021/acsapm.6c00522
ACS Appl. Polym. Mater. 2026, 8, 8183−8197

showed an approximately concentration-independent fraction of free counterions, and the effective charge was similar to the Oosawa-Manning threshold. Beyond a critical concentration, counterion condensation increased with increasing concentration, which was assigned to a crossover to the concentrated regime. Scattering data for CMC[83] and polystyrenesulfonate (PSS)[84] with organic counterions suggest counterion delocalization at high polymer concentrations, which appears inconsistent with increased condensation. The complex permittivity of NaCMC solutions at intermediate frequencies followed scaling laws with concentration similar to those of flexible polyelectrolytes.[85] The fraction of free counterions estimated by applying the scaling model to dielectric increment data gave a similar result to that obtained from electrical conductivity (see ref 80).

The electrical conductivity of sodium carboxymethyl cellulose in DI water solutions and mixtures of water and organic solvents has been investigated extensively by Das and Nandi[86−93] who applied the model of Colby et al.[85,94] to calculate the fraction of free counterions as a function of the degree of substitution, polymer concentration, and nonsolvent fraction. One limitation of these works is that, in order to calculate the correlation length—which is needed to fit the model of Colby et al. to conductivity data—the authors relied on the scaling theory for flexible polyelectrolyte solutions. In their calculation, they assume chain flexibility on length scales larger than the chemical monomer size (≃0.5 nm), which is unrealistic for a semiflexible polymer like CMC. In a recent study, we measured the correlation length using SAXS[49] in water and water/nonsolvent mixtures, which allowed us to more directly calculate the fraction of free counterions. The results showed that the fraction of charged monomers was nearly independent of polymer concentration and inversely proportional to the Bjerrum length, as anticipated by the Oosawa-Manning theory, but the charge density was found to be ≃1.5× lower than the OM threshold.

1.1.2. Solution Structure and Rheological Properties. Several studies employing scattering methods[49,62,83,95,96] have shown that the local conformation of NaCMC in water is rod-like, as expected due to the semiflexible nature of the cellulose backbone. The scattering patterns of alkaline salts in aqueous solutions display a correlation peak, characteristic of salt-free polyelectrolyte solutions, over the entire concentration range studied. The correlation length (ξ) was found to be proportional to $c^{-1/2}$, in agreement with the prediction of the scaling theory.[46,97] For tetra-alkyl-ammonium salts of CMC, the SANS spectra display a peak at low concentrations that morphs into a broad shoulder feature as the concentration is increased. The SAXS signal, on the other hand, showed clear peaks over the entire concentration range, following the $\xi \propto c^{-1/2}$ dependence. Because the SANS signal is dominated by the counterion contribution, this likely results from a decoupling of the polymer backbone and counterion concentration fluctuations, a feature that has been observed, albeit to a smaller extent, for TMAPSS in water.[84]

The structure of NaCMC and CsCMC in mixtures of water and ethanol, 2-propanol, and acetone was studied by small-angle X-ray scattering.[49] The addition of a nonsolvent decreased the effective charge of the backbone, but the correlation length was independent of solvent composition except when solutions were close to the solubility boundary. The independence of the scattering peak on the effective charge fraction of the chain is expected by the scaling model when the bare Kuhn segment of the chain (≃10 nm for NaCMC) is much larger than the Bjerrum length of the solvent (≃1−2 nm for the solvent mixtures studied).[49]

Other studies on the behavior of NaCMC in mixed solvents have focused on understanding the rheological properties of solutions.[98−102] Rozanski and coworkers showed that, for sufficiently high polymer concentrations and/or low degrees of substitution, addition of a nonsolvent can lead to a sol−gel transition.[100,101] The nonsolvent-induced gelation likely arises from a combination of two phenomena: first, as a nonsolvent is added and the effective charge of the backbone decreases, the energetic barrier for two segments to approach each other decreases, thereby facilitating interchain associations. Second, as the solvent quality worsens, unsubstituted regions of the cellulose backbone experience stronger attractions.[101]

In this paper, we study the scattering properties of TBACMC in several organic solvents and water. The scattering data are used in combination with electrical conductivity measurements to estimate the fraction of free counterions over a relatively broad range of dielectric permittivities. Our results show reasonable agreement with the Oosawa-Manning condensation threshold and yield new insights into the spatial correlations between monomers and counterions.

2. SCATTERING OF POLYELECTROLYTE SOLUTIONS

The SANS or SAXS intensity of a polyelectrolyte solution can be expressed in terms of the structure factors of the monomers and counterions as[103]

$$I(q) = \rho_m \overline{b}_m^2 S_{mm}(q) + 2\sqrt{\rho_m \rho_c}\,(\overline{b}_m \overline{b}_c) S_{mc}(q) + \rho_c \overline{b}_c^2 S_{cc}(q) \tag{2}$$

where $S(q)_{mm}$, $S(q)_{mc}$, and $S(q)_{cc}$ are the partial structure factors for monomer−monomer, monomer−counterion, and counterion−counterion correlations, respectively. The concentrations, in units of number per unit volume, are ρ_m and ρ_c, where the m subscript refers to the monomer and the c subscript refers to the counterion (see refs.103,104 for details).

The contrast factors in eq 2 are

$$\overline{b}_i = b_i - b_s \frac{v_i}{v_s} \tag{3}$$

where b_i and v_i are the coherent scattering length and volume of the unit, respectively. The coherent scattering length is the sum of the coherent scattering lengths of each isotope in the scattering unit. For SANS, values of b_i were taken from the NIST website.[105] For SAXS, b_i is the product of the number of electrons of the scattering unit and the electron scattering length. The subscript s refers to the solvent, and i = c or i = m refers to the counterion or monomer.

In an earlier study[83] we estimated the molar volumes of the TBA^+ and CMC^- from density measurements. However, these calculations did not take into account electrostriction of the solvent. Here, we use a molar volume of 274 mL/mol for the TBA^+ ion, following ref 106, and 134 mL/mol for the CMC^- ion. SANS experiments were conducted using deuterated solvents, and for all systems studied the prefactor to the counterion structure factor $\left(\rho_c \overline{b}_c^2\right)$ dominates over the backbone's $\left(\overline{b}_m^2\right)$. For the solvents studied with SAXS, the opposite is true, and the prefactor to $S(q)_{mm}$ is 2−3 orders of magnitude larger than for $S(q)_{cc}$.

https://doi.org/10.1021/acsapm.6c00522
ACS Appl. Polym. Mater. 2026, 8, 8183−8197

3. MATERIALS AND METHODS

3.1. Materials

NaCMC was purchased from Sigma-Aldrich, with a nominal molar mass of 250 kg/mol and a degree of substitution (DS) ≃ 1.2. The molar mass of the sodium salt was determined from the intrinsic viscosity in 0.1 M NaCl to be ≃240 kg/mol in earlier studies.[107,108] The degree of substitution was measured by back-titration of the acid form as DS = 1.3. Spectra/Por dialysis membranes with a MWCO of 6−8 kDa were used and were purchased from VWR. Solvents were purchased from VWR or Sigma-Aldrich, except for *n*-methyl formamide (NMF), which was from FUJIFILM Wako Pure Chemical Corporation. Deuterated solvents for the SANS experiments were purchased from Deutero GmbH (Germany). The purity for each solvent is listed in Table S2.

3.2. Preparation of CMC Salts

NaCMC was dialyzed against DI water and freeze-dried. The freeze-dried polymer was used to prepare the NaCMC solutions. The TBACMC used in this study is the same as that in our previous work (see ref 83). In brief, the NaCMC was converted to its acid form (HCMC) by adding excess HCl, followed by dialysis against DI water. The HCMC was freeze-dried, neutralized with excess TBAOH, dialyzed against DI water, and freeze-dried.

3.3. Sample Preparation

The dialyzed and freeze-dried CMC salts were stored in the vacuum freeze-dryer for ∼24 h before any samples were prepared. The samples were prepared in polypropylene microcentrifuge tubes, which had been previously washed with DI water and dried at 60 °C. All the sample components were added by weight using a weighing balance with a least count of 0.1 mg and, therefore, a typical error of ± 0.05 mg. Solvents were used as received, without further purification.

3.4. Densitometry

The density measurements were performed using the Anton Paar DMA 5000 densitometer with a least count of 10^{-6} g cm^{-3}. The accuracy of the instrument was checked using DI water.

3.5. Conductivity and pH

Conductivity measurements were made using the Mettler Toledo S47 SevenMulti conductivity meter. The temperature was maintained at 25 ± 0.1 °C using a continuously stirred water bath and heating plate system provided with temperature probes at different points to ensure temperature accuracy. Upon achieving the required temperature, the mean value of four measurements was taken. pH measurements were made using the Metrohm 744 pH meter. For measurements in NMF, the TBACMC was added to the as-received solvent, and dissolution occurred within 1 h. Several solutions of lower concentrations were prepared by dilution, and the conductivity for each was measured immediately after each solution was prepared. The conductivity for each concentration was measured again approximately 48 and 96 h later to assess if significant quantities of residual ions from the air or the containers were absorbed by the solution, thus affecting their conductivity readings.

3.6. Small-Angle Neutron Scattering

The SANS measurements were carried out at the D11 beamline at Institut Laue Langevin, Grenoble, France. Measurements were performed at five different sample-to-detector distances (1.7 m, 5.5 m, 8 m, 12 m, and 28 m), depending on the sample, covering a *q*-range of 0.002−0.55 $Å^{-1}$. The neutron wavelength was λ = 6 Å for all experiments. Samples were measured in cylindrical (banjo) cells with path lengths of 1 mm, 2 mm, or 5 mm, depending on polymer concentration. The reduced scattering intensities are tabulated in the Supporting Information. All samples for the SANS experiment used deuterated solvents. The grade for each solvent is listed in ref 109.

3.7. Small-Angle X-ray Scattering

The SAXS measurements were carried out using an in-house instrument and at the SPring-8 synchrotron. The in-house instrument consists of a 3-pinhole S-Max3000 system with a MicroMax002+ X-ray microfocus generator from Rigaku and a 2D multiwire detector with an active diameter of 200 mm. A sample-to-detector distance of 2.6 m was used, which covered a *q*-range of 0.005−0.4 $Å^{-1}$ (λ = 1.54 Å, Cu radiation). The samples were measured in sealed 1.5 mm borosilicate capillaries from WJM Glas Müller GmbH. Measurements at the BL40 beamline of the SPring-8 synchrotron facility (Hyogo, Japan) followed the same procedure as in our previous study (see ref 83) for details. 2 mm capillaries were used, and acquisition times were generally between 20 s and 2 min, depending on solvent and polymer concentration. The sample-to-detector distance was set to 1 or 2 m. The reduced scattering intensities, in arbitrary units, are tabulated in the Supporting Information for all measurements.

All the data were acquired at 25 °C except for measurements in NMA, which were performed at 35 °C to be above its melting point. Measurements of the dialysis bath conductivity were performed at room temperature (≃22 °C).

The concentrations (c) reported in the paper are expressed as the number of monomers (repeating units) per unit volume. The unit *M* stands for moles of monomers per liter of solution.

4. RESULTS AND DATA FITTING

4.1. Solvent Properties and Conductivity Measurements

Viscosity, conductivity, and density values for the various solvents used in this study are listed in Table S1. The densities measured in our laboratory agree with literature values within a few percent, as expected for the solvent grades used. All the solvents have relatively low conductivities, with the exception of NMF, which is known to have a relatively high content of ionic impurities.[110−112] For deionized water, a conductivity of ≃2 μS/cm is usually taken to correspond to a residual salt concentration of ≃4 × 10^{-6} M, estimated from the pH of the solution.[113] Lacking information on the type of ionic impurities in our samples, we assume they are common monovalent salts such as alkaline halides. Such monovalent ions usually have limiting ionic conductances of $\lambda \simeq 6 \pm 1$ mS m^2/mol and the conductivity of a 1 mM solution is ≃150 μS/cm.[114] An approximate value for the residual salt concentration (c_{res}) can be obtained by assuming the conductivity to be proportional to c_{res} and inversely proportional to the solvent's viscosity:

$$c_{res}[\mathrm{mM}] \simeq \frac{\eta_{solvent}}{\eta_{water}} \frac{\sigma_{solvent}}{150} \tag{4}$$

where $\eta_{solvent}$ and σ are the viscosity and conductivity in μS/cm of the solvent, respectively.

The residual salts for the various solvents studied, calculated using eq 4, are listed in Table S1. For most solvents, the residual salt concentration is in the range of a few micromolar. *N*-Methyl-formamide and *N*-methyl-acetamide (NMA) have higher c_{res}, approaching the millimolar range. For a discussion of impurities in NMF (see ref 111).

The specific conductance ($\Lambda = \sigma/c$) showed a weak concentration dependence in all solvents, in agreement with earlier reports for alkaline salts of CMC in water or water/nonsolvent mixtures.[89−91,93,115] Conductivity data are tabulated in the Supporting Information.

4.2. Small-Angle X-ray Scattering

The small-angle X-ray scattering patterns of TBACMC in high dielectric constant solvents—NMF, NMA, and water—are plotted in Figure 1. In NMF solutions, a correlation peak is observed for all concentrations. This feature is characteristic of polyelectrolytes in low ionic strength solvents and confirms the relatively low content of ionic impurities of the NMF used in

https://doi.org/10.1021/acsapm.6c00522
ACS Appl. Polym. Mater. 2026, 8, 8183−8197

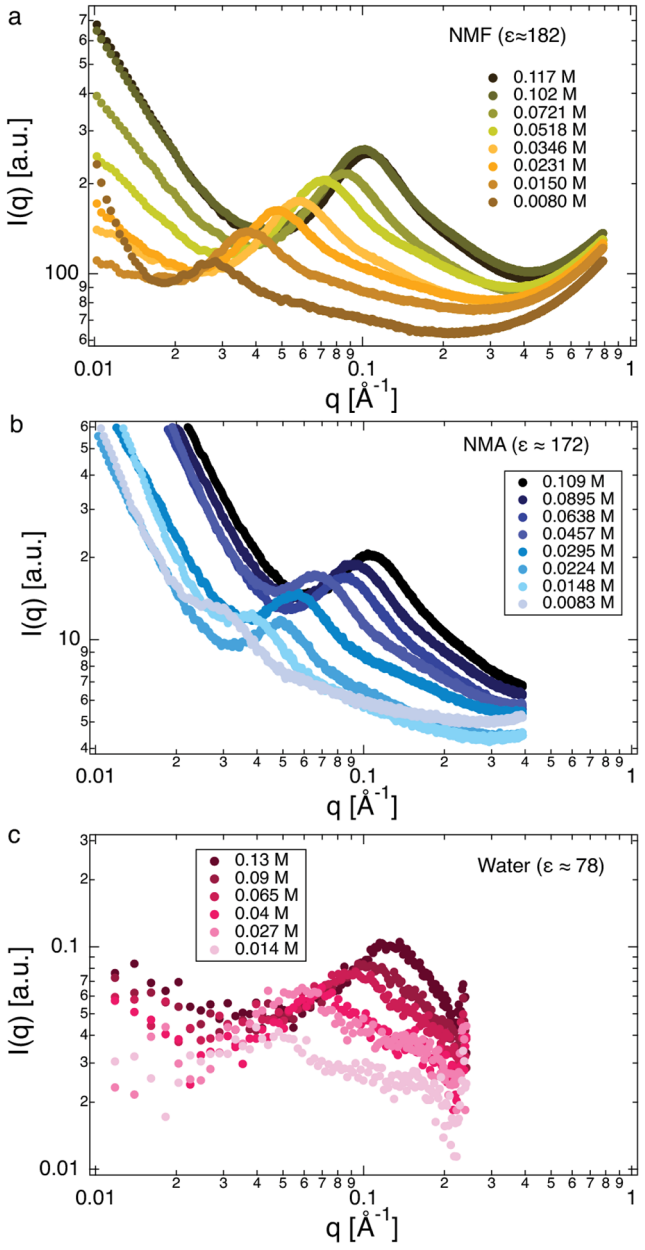

Figure 1. SAXS profiles for TBACMC solutions in high dielectric constant solvents: *N*-methyl formamide (ϵ = 182, l_B = 0.3 nm at T = 25 °C) (a), *N*-methylacetamide (ϵ = 178, l_B = 0.31 nm at T = 35 °C) (b), and water (ϵ = 78, l_B = 0.71 nm at T = 25 °C) (c). Data for aqueous solutions are from ref 83., binned (3 to 1) for clarity. Note that the *x*-axis has the same range for all panels.

this study. For *N*-methyl-acetamide, the correlation peak is not observed for the lowest concentration measured, and the scattering profile instead displays a shoulder. This can be assigned either to the presence of residual salts or to the contribution from the low-*q* upturn, which masks the peak. The former scenario would imply a residual salt concentration of $c_S \simeq 0.01$ M (see Figure 3 and related discussion) and is incompatible with the relatively low conductivity of the NMA used (see Table S1).[116] For the aqueous solutions, the data display a correlation peak over the entire concentration range studied, which is consistent with the high dielectric constant of water and its low residual salt content.

Figure 2 shows SAXS data for TBACMC solutions in three linear alcohols: methanol ($\epsilon \simeq 32$), ethanol ($\epsilon \simeq 24$), and 1-propanol ($\epsilon \simeq 22$). The methanol and ethanol data are measured with the Rigaku in-house instrument. The acquisition times are a few hours, depending on the concentration. Despite the relatively large scatter, the high point density around the maxima means that the peak position can be extracted accurately. The 1-propanol solution data, measured at the SPring-8 synchrotron (45−120 s), display considerably less scatter than the samples measured in-house

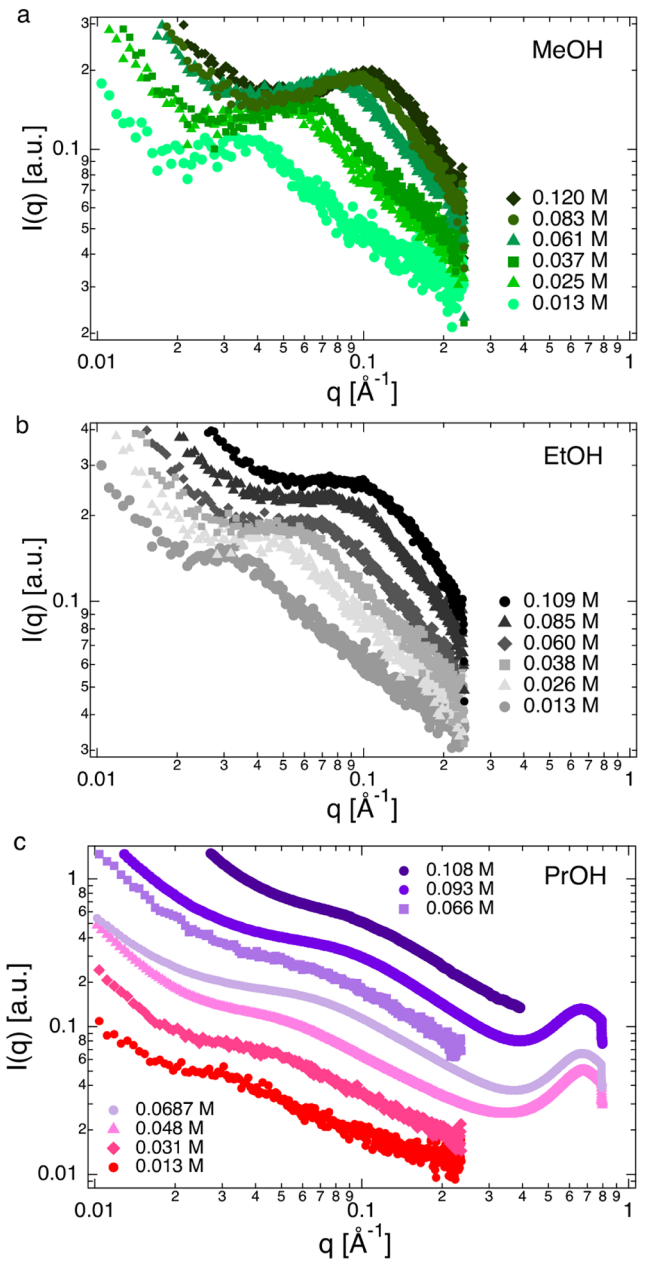

Figure 2. SAXS profiles for TBACMC solutions in methanol (MeOH), ethanol (EtOH), and 1-propanol (PrOH). Concentrations are indicated in the legends. Methanol and ethanol data are measured on the in-house Rigaku instrument. Propanol data are measured on the Rigaku instrument (c = 0.014, 0.033, and 0.071 M) or at the SPring-8 synchrotron (c = 0.111 M measured with a 2 m configuration, others with a 1 m configuration). All data are in arbitrary units. Note that the *x*-axis has the same range for all panels.

https://doi.org/10.1021/acsapm.6c00522
ACS Appl. Polym. Mater. 2026, 8, 8183−8197

due to the much higher flux of the X-ray beam. The scattering patterns for solutions in methanol display a clear peak over the entire concentration range. For ethanol solutions, the peak at low concentrations morphs into a shoulder at high concentrations, and for 1-propanol solutions, no polyelectrolyte peak is observed at any concentration (the peak at $\simeq$ 0.6 Å^{-1} arises from the solvent contribution and not from the polyelectrolyte chains). Instead, all samples display a broad shoulder and an upturn at low wave-vectors.

4.2.1. Effect of Added Salt on the Polyelectrolyte Peak. The scattering properties of NaCMC solutions in aqueous NaCl solutions were studied as a function of added NaCl concentration. The results are shown in Figure 3. As the

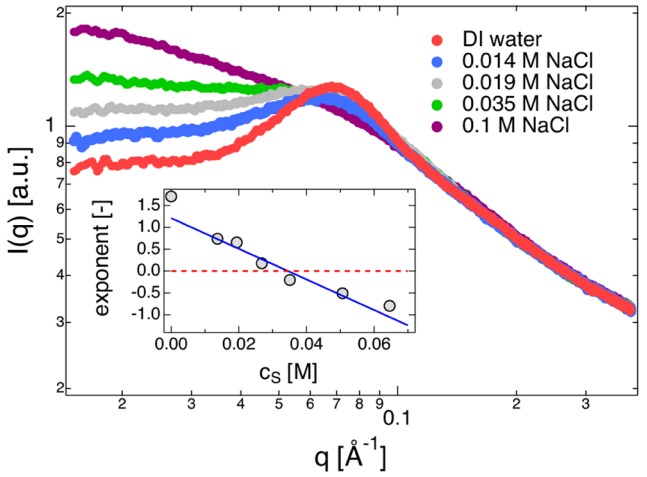

Figure 3. SAXS curves for NaCMC at c = 0.054 M with different added NaCl concentrations, indicated in the legend. The exponents for $q \lesssim q^*$ are plotted as a function of added NaCl in the inset. For $c_S \simeq$ 0.035 M, the exponent is approximately zero, which we identify as the transition between peak and shoulder regimes.

NaCl concentration increases, the peak first becomes broader and then disappears. We fit power laws to the $q \lesssim q^*$ and $q \gtrsim q^*$ regions, where q^* is the position of the maxima in salt-free solutions. The exponent in the high-q region is independent of c_S, and the exponent in the low-q region (m_l) increases with increasing c_S, as shown in the inset. The point at which $m_l = 0$ can be identified as the transition point between peak and shoulder behavior. This crossover occurs when $2c_S/(fc) \simeq 2.5$, in qualitative agreement with the scaling model.[46] Results for polystyrenesulfonate[117−119] show a similar value of $fc/(2c_S) \simeq 3$.[80,85,120]

4.3. Small-Angle Neutron Scattering

Figure 4 plots the SANS scattering intensity of TBACMC in different solvents for a range of concentrations. There are three types of relationships observed between concentration and peak sharpness. In dimethyl sulfoxide (DMSO), the peaks are distinct for all the concentrations studied. The more common behavior, observed for water, ethanol, and methanol, is that the peak disappears at higher concentrations. For dimethylformamide (DMF), the peak is prominent at high concentrations but vanishes at lower concentrations. We did not measure the conductivity of the deuterated DMF and, therefore, cannot clearly resolve if the disappearance of the peak at low polymer concentrations is the result of a crossover to the high-salt regime. Common grades of hydrogenated DMF with comparable purity to the deuterated DMF used (99.5%) display low conductivities, corresponding to residual salt concentrations of a few micromolar, which are not sufficient to explain the peak disappearance at around $c \simeq$ 0.008 M (see Table S1). The same holds for ethanol solutions.

We extracted the peak positions by fitting a polynomial around the local maxima in the scattering intensity. When no clear maximum is observed, we fit two linear functions and use their intercept as the position of the scattering shoulder.[83,121] An alternative approach to fitting the data, where the low-q upturn is fit simultaneously with the peak, is considered in the Discussion Section.

5. DISCUSSION

5.1. Solution Structure

The correlation length of a salt-free polyelectrolyte solution is predicted by the scaling theory to be:[1]

$$\xi = \left(\frac{B}{bc}\right)^{1/2} \tag{5}$$

where b is the monomer length ($\simeq$5.15 Å for cellulose polymers), B is the stretching parameter, which describes the extent of chain folding inside a correlation blob: $B = 1$ corresponds to a fully stretched conformation inside the correlation blob, and $B > 1$ indicates chain folding corresponding to an effective monomer size of b/B, and c is the number concentration of repeating units.[46] Each correlation blob contains g_ξ monomers:

$$g_\xi \simeq B\xi/b \tag{6}$$

The correlation length can be measured from the position of the peak or the shoulder in the scattering function (q^*) as:

$$\xi = 2\pi/q^* \tag{7}$$

5.1.1. Decoupling of Backbone and Counterion Fluctuations. The peak positions in the SANS and SAXS spectra of TBACMC in H_2O, MeOH, and EtOH are plotted as a function of $c^{1/2}$ in Figure 5. For all three solvents, the SAXS peak positions, which approximately correspond to the maxima in $S(q)_{mm}$, follow a power law of $q^* \propto c^{1/2}$, as expected by eqs 5 and 7. For H_2O and MeOH, the maxima in $S(q)^{cc}$, measured by SANS, agree with $S(q)_{mm}$ measured by SAXS at low concentrations, but q^* at intermediate and high concentrations deviate to lower values. As before, we interpret this as resulting from a decoupling of the length scales over which the polymer backbone and the counterions fluctuate. This is not observed for solutions in ethanol, for which the values of q^* measured by SANS and SAXS agree over the entire concentration range. However, while the SAXS signal displays a clear peak over the entire concentration range studied, the SANS signal displays a shoulder for $c \gtrsim$ 0.05 M. Therefore, even though both monomer and counterion fluctuations occur over similar length scales, the counterions appear to be less strongly correlated than the monomers for this system. For DMF solutions, SAXS data showed shoulders over the entire concentration range measured, while SANS data showed clear peaks except at the low concentrations. The reason for this behavior remains unclear.

In an earlier study on aqueous CMC solutions,[83] we observed that concentration fluctuations between backbone and counterions decouple at high concentrations for tetraalkylammonium salts of CMC but not for alkali salts. The

https://doi.org/10.1021/acsapm.6c00522
ACS Appl. Polym. Mater. 2026, 8, 8183−8197

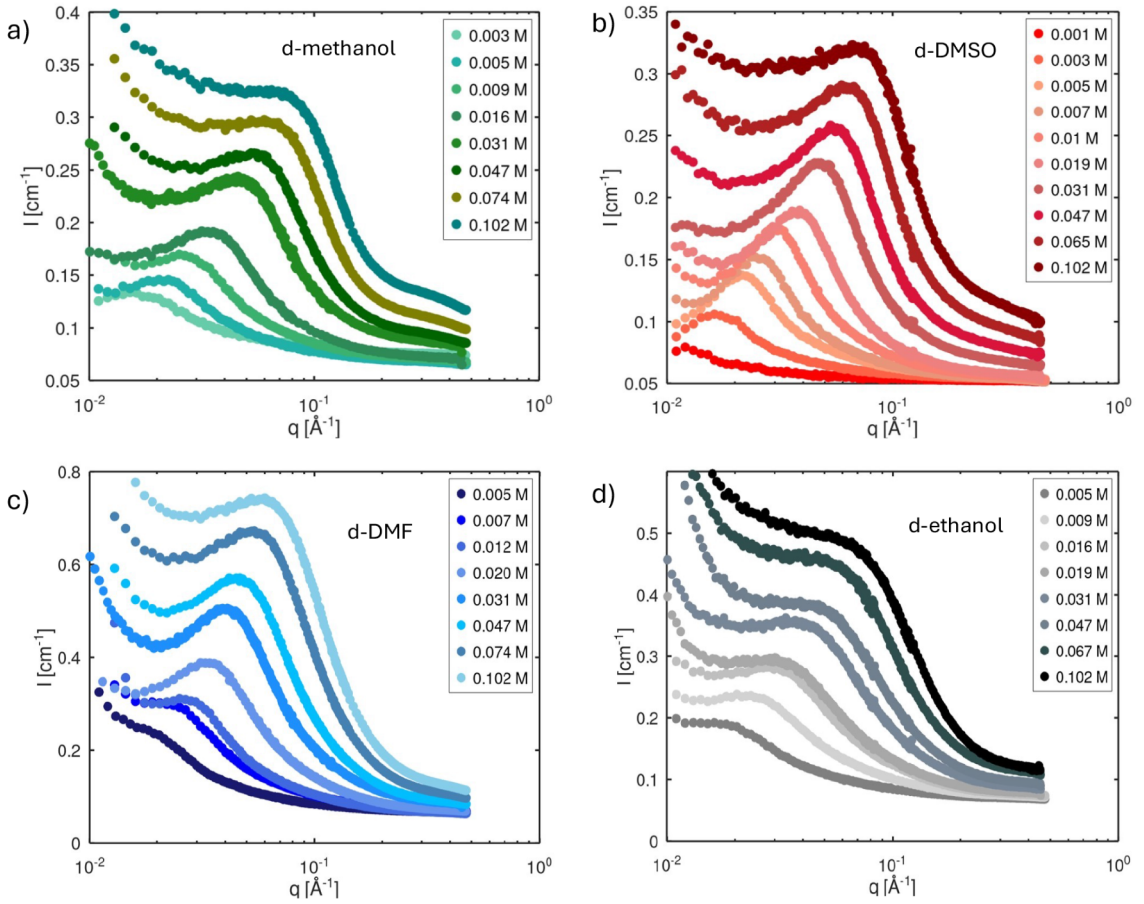

Figure 4. SANS intensity I as a function of scattering wavevector q for TBACMC in methanol (MeOH), dimethyl sulfoxide (DMSO), dimethylformamide (DMF), and ethanol (EtOH) at different concentrations, indicated in the legends. All solvents are deuterated.

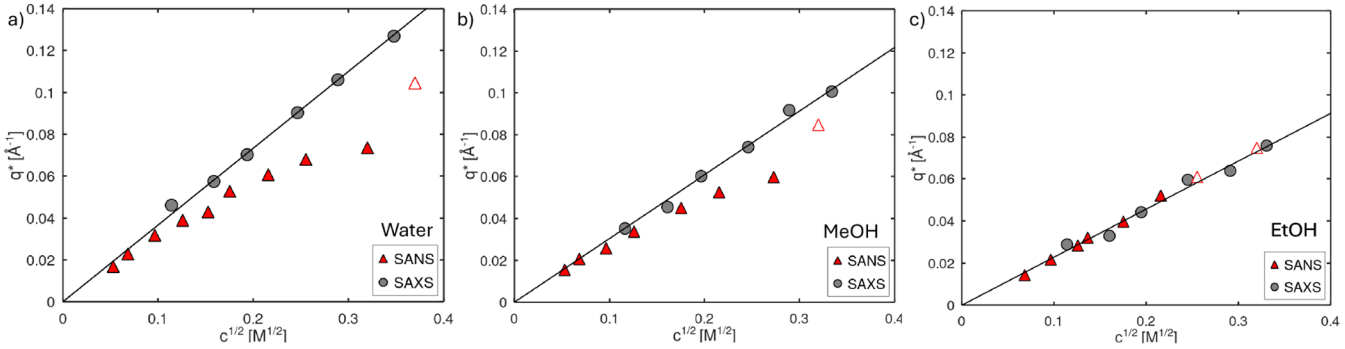

Figure 5. Peak or shoulder positions (q^*) as determined from I vs q curves (SANS: triangles, SAXS: circles) for TBACMC in (a) water ($\epsilon \simeq 78$), (b) methanol ($\epsilon \simeq 32$), and (c) ethanol ($\epsilon \simeq 24$) as a function of concentration. Full symbols represent samples displaying a peak, and hollow symbols represent samples displaying a shoulder. Lines are fits to SAXS data (water and MeOH) and to SANS and SAXS data (EtOH). The best-fit values give $B \simeq 0.85$ (water), $B \simeq 1.4$ (methanol), and $B \simeq 2.5$ (ethanol).

decoupling was more pronounced for larger tetra-alkylammonium (TAA) salts. The fractions of dissociated counterions for both salts are nearly identical (see discussion below). The decoupling could then be assigned to the solvophobic nature of the TAA ions, but it seems counterintuitive that solvophobic ions should be more delocalized from the backbone, thereby maximizing contacts with the solvent. In any case, if the counterion-solvent interactions play a role in delocalization, the results in Figure 5 could be assigned to differences in the solvation of the TBA^+ ion by ethanol compared to water and MeOH. Alternatively, the higher fraction of condensed counterions for ethanol relative to that for water and methanol may oppose the decoupling of concentration fluctuations between monomers and counterions. SANS and SAXS data for TBAPSS in water show a much weaker decoupling than that for TBACMC, presumably due to the higher fraction of condensed counterions.

Decoupling of polymer and counterion concentration fluctuations at high concentrations has been reported previously. Combet et al.[84] observed that the peak in $S(q)_{cc}$ matches that of $S(q)_{mm}$ at low concentrations but takes a lower value at high concentration, in line with the results reported

https://doi.org/10.1021/acsapm.6c00522
ACS Appl. Polym. Mater. 2026, 8, 8183−8197

Table 1. Properties of TBACMC in Various Solvents[g]

Solvent	l_B [nm]	B	Λ(0.065M) [S cm^2]	λ_C [mS cm^2/mol]	$\lambda_C\eta_s$ [10^{-2} NsS/mol]	f_{exp} [−]	f_{exp}/f_{OM}[a] [−]
NMA (T = 35 °C)	0.31	1.17	3×10^{-3}	6.85[b]	23.5	0.73	0.43
NMF	0.31	1.25	1.1×10^{-3}	14[c]	23.5	0.67	0.4
Water	0.71	$\simeq 1$[d]	4.0×10^{-3}	19.47	17.4	0.61	0.85
DMSO	1.19	(1.2)[a]	1.3×10^{-3}	9.23	23.2	0.35	0.78
Ethylene glycol (EG)	1.5	(2.3)[e]	1.6×10^{-4}	1.51	25.1	0.27	0.67
DMF	1.5	(1.6)[a]	1.2×10^{-4}	22.90	21.05	0.24	0.66
Methanol	1.71	1.4	6.1×10^{-4}	39.08	21.3	0.31	0.95
Ethanol	2.24	2.4	2.6×10^{-4}	19.74	21.4	0.15	0.65
1-Propanol	2.72	$\simeq 2$[f]	-	11.0	21.42	-	-

[a]Value estimates by linearly extrapolating B calculated from SANS data to c = 0 (see the text). For DMF, the value calculated from the position of the SAXS shoulders is B = 1.8. [b]Calculated using data from refs.[131,132] assuming that the Walden product at 35 °C and 40 °C is the same. [c]From ref 133. [d]Value for NaCMC. For TBACMC, the best-fit SAXS results in ref 83. give $B \simeq 0.85$, which is unphysical. Hou et al's measurements for TBACMC give $B \simeq 1$.[57]. [e]The average value was obtained from four SANS measurements. [f]None of the samples measured showed peaks. [g]f_{OM} is the fraction of charged monomers expected by the Oosawa-Manning model and f_{exp} is the value determined from eq 8

here for TBACMC. A similar trend can be observed by comparing SAXS data by Nishida et al.[122] and SANS data by Douglas et al.[123] for aqueous NaPSS. The SANS measurements, dominated by backbone contrast, show $\xi \propto c^{-1/2}$ up to 3 M, whereas SAXS exhibits a crossover from $c^{-1/2}$ below 1.3 M to $c^{-1/4}$ at higher concentrations, likely because sodium counterions contribute more strongly to the SAXS contrast than to SANS.

5.1.2. The Stretching Parameter. To calculate the stretching parameter B for TBACMC, the q^* value of $S(q)_{mm}$ should be employed. In order to estimate this, we used the following approach: for H_2O, MeOH, EtOH, NMF, and NMA, the q^* values in the SAXS profiles, which are our best estimate for $S(q)_{mm}$, are used to calculate the correlation length. For methanol and water, plotting the stretching obtained from SANS and SAXS peaks as a function of concentration, it is observed that the values obtained from the two techniques converge at low polymer concentrations. We therefore use this method for DMSO and DMF, for which we lack SAXS measurements of the correlation length. The best-fit values of the stretching parameter are listed in Table 1.

The scaling theory models the conformation inside a correlation blob as a pole of electrostatic blobs of size ξ_{el}. Inside the electrostatic blob, the conformation is unaffected by electrostatic interactions. On distances larger than ξ_{el}, electrostatic repulsion strongly stretches the chain. For flexible polymers, as the effective charge of the backbone decreases, the size of the electrostatic blob increases, allowing for greater chain folding inside the correlation blob, which results in higher values of the stretching parameter.[130] For semiflexible chains, where the bare (intrinsic) Kuhn segment is much larger than ξ_{el}, chains cannot fold inside the electrostatic blob. The electrostatic blob size is predicted to be of the order of the Bjerrum length when there is more than one dissociated counterion per Kuhn segment.[17,46] In this case, the stretching parameter should be charge-independent and close to unity. Experimental results for semiflexible polyelectrolytes support this, as shown in Figure 6. Note that the data presented in this figure are for sodium salts of various polyelectrolytes, and therefore the contrast arises primarily from the polymer backbone. The correlation length of double-stranded DNA and several polysaccharides follows a scaling law of $\xi \simeq (bc)^{-1/2}$, corresponding to eq 5 with B = 1.

Figure 7 plots the stretching parameter as a function of the fraction of monomers with a dissociated counterion, where f is

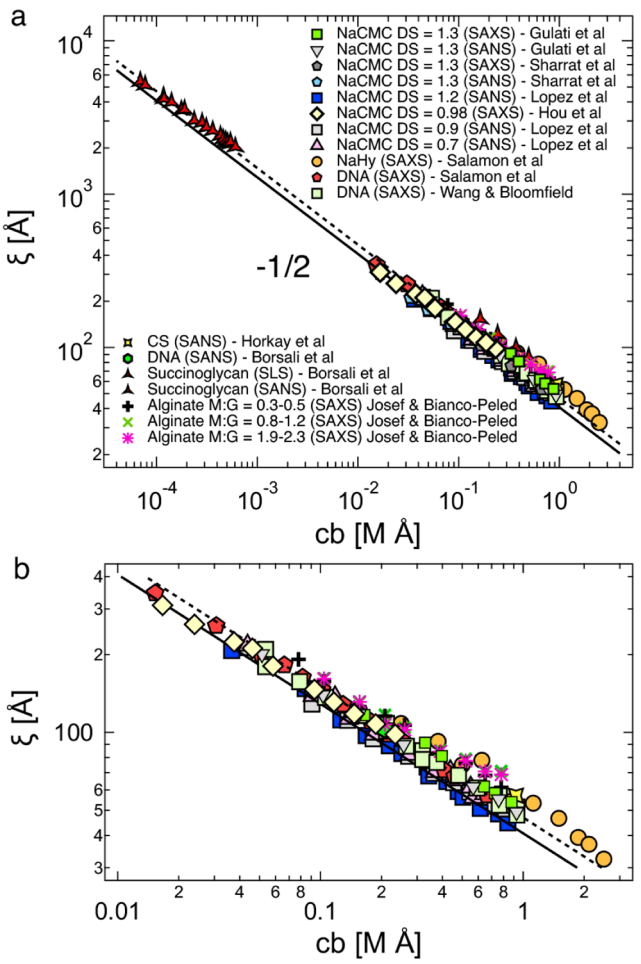

Figure 6. Correlation length of semiflexible polyelectrolytes in salt-free water as a function of polymer concentration multiplied by monomer size. Data are from refs.[49,62,83,95,96,121,124−128] (see legend). Part b zooms into the high-concentration regime. The full line represents scaling theory with B = 1, and the dashed line represents Koyama's prediction.[129] The monomer length is b = 5.15 Å for polysaccharides and 3.4 Å for double-stranded DNA. CS is for chondroitin sulfate. M:G is the ratio of mannuronic acid to guluronic acid in alginate.[49]

obtained from conductivity as discussed below. For NMA, NMF, water, and DMSO ($l_B \simeq 0.3$−1.2 nm), the stretching parameter B takes a value close to unity. For DMF, ethylene

https://doi.org/10.1021/acsapm.6c00522
ACS Appl. Polym. Mater. 2026, 8, 8183−8197

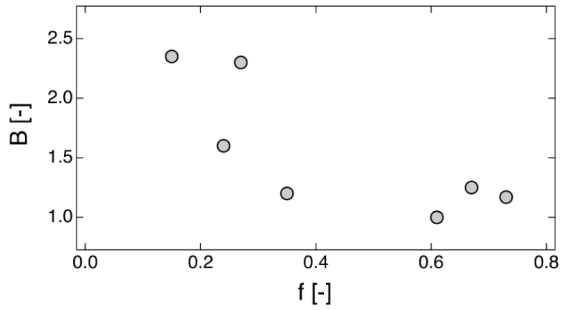

Figure 7. Dependence of the stretching parameter on the effective charge of the CMC backbone. The values of f are calculated from conductivity and scattering data, as discussed in section 5.1.4.

glycol, methanol, and ethanol, the higher values of B imply some degree of folding inside the correlation blobs. This result is only expected from the scaling model if the Kuhn segment is smaller than the electrostatic blob. For CMC, the intrinsic Kuhn length in water is $l_{K,0} \simeq 10$ nm.[108] Values of $l_{K,0}$ in other solvents have not been reported, but it seems unlikely that it will be smaller than 1−2 nm as required for $l_{K,0} \lesssim \xi_{el}$. Alternatively, changes in B may not be related to the electrostatic blob size and instead reflect the solvent-dependent local conformation of the cellulose backbone. In this case, the correlation of B with f would be coincidental.

5.1.3. Influence of Solvent Properties on Peak Sharpness. Figure 8a compares the SANS curves of TBACMC solutions at a concentration of c = 0.033 M in methanol, ethanol, and 1-butanol. A clear peak is observed for the solution in methanol. In ethanol, a similar but broader peak is observed, and the 1-butanol solution displays a shoulder feature. The scaling model explains the presence of the correlation peak in polyelectrolyte solutions as follows: the large osmotic pressure generated by free counterions suppresses long-ranged concentration fluctuations in polyelectrolyte solutions, generating a correlation hole at low q and the maximum in the structure factor of salt-free polyelectrolyte solutions. More specifically, the scaling theory predicts that, for solutions without added salt, the structure factor displays a peak if there is more than one dissociated charge per correlation blob. This appears to be inconsistent with the results reported here: in 1-propanol solutions, no peak is observed for concentrations as low as 0.014 M ($\xi \simeq 20$ nm, $g_\xi \simeq 90$). By contrast, in methanol a peak is observed at c = 0.11 M ($\xi \simeq 6$ nm, $g_\xi \simeq 17$). This would imply that f for methanol should be ≃×5 higher than in 1-propanol, which seems unreasonable given that the dielectric constant is only ≃×1.5 lower.

The theory of Koyama[129] explains the peak as arising from the strong repulsion between like-charged polymer segments, which induces local ordering. Koyama's theory predicts a peak for neutral polymer solutions if the repulsive interactions between chains are sufficiently strong. As the Bjerrum length of the solvent increases, the effective charge of the backbone decreases, which weakens electrostatic repulsions between like-charged segments. However, the Coulomb potential between two charges increases proportionally to the Bjerrum length. Therefore, it is not clear if the results in Figure 8 can be accounted for by invoking Koyama's model.

A third possible explanation for the disappearance of the peak is the stronger low-q upturn. For the SAXS measurements, the contribution from the capillary background is too

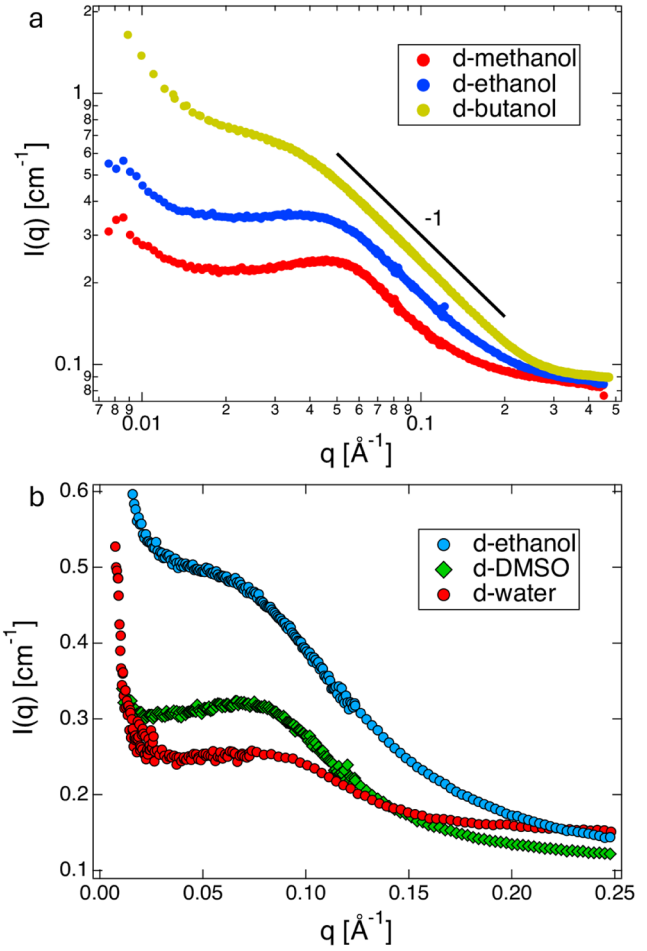

Figure 8. (a) SANS curves for c = 0.031 M solutions of TBACMC in three linear alcohols. The solid line represents a power law with an exponent of −1. (b) SANS intensity I as a function of scattering wavevector q for TBACMC in water, DMSO, and EtOH at c = 0.102 M, showing an observable difference in correlation peak sharpness.

strong at low q, preventing us from resolving this upturn. In the SANS experiments, the measured q-range did not extend sufficiently far into the low-q regime to capture the upturn well. When we fit a power law to the low-q region ($I(q)_{upturn} \propto q^{-1.4}$ over the limited q-range studied) and subtract this contribution from the total scattering signal (see figure S1), a peak becomes apparent, the position of which is usually not very different from that obtained by fitting two power laws to the unsubtracted signal. The appearance of the peak in the subtracted signal may be an artifact of the subtraction procedure. Additionally, we note that experiments where the low-q upturn is fitted over a broader q-range typically display a stronger power-law exponent than our fit over a limited q-range. Data for aqueous solutions provide evidence against the low-q upturn being the cause of the peak disappearance. For aqueous solutions at modest concentrations, the low-q upturn is much stronger for NaCMC than for TBACMC (see Figure 5 of ref 83); however, NaCMC displays a clear correlation peak but TBACMC does not.

Figure 8b compares the SANS profiles of TBACMC at a concentration of c = 0.11 M in the three solvents. The curve for DMSO displays a sharper peak than that in water. In the case of ethanol, no maximum in the scattering intensity is observed and only a broad shoulder is apparent, indicating a

https://doi.org/10.1021/acsapm.6c00522
ACS Appl. Polym. Mater. 2026, 8, 8183−8197

broader (less localized) distribution of counterions. Note that for ethanol, the SAXS data also show a broad shoulder at high concentrations, indicating less order for the polymer backbone. As discussed above, the scaling theory expects peak sharpness to correlate with the charge density of the polymer, with higher charge densities resulting in sharper peaks, which is not observed here.

In conclusion, the dependence of several features observed in the scattering patterns across different solvents is not easily explained by any of the models considered and likely reflects the complex nature of polyelectrolyte solutions, which is not captured by existing models.

5.1.4. Comparison with the Behavior of Flexible Polyelectrolytes. In two earlier studies on the scattering properties of flexible polyelectrolytes[20,134] we observed that for solvents of low dielectric constant, the scaling of the correlation length with concentration follows $\xi \propto c^{-1/3}$. We interpreted this as arising from the chain collapse into a pearl-necklace structure. The collapse can be driven by solvophobic forces or attractive forces between condensed counterions. The results presented here for CMC do not show any indication of polymer collapse, and the scaling of $\xi \propto c^{-1/3}$ is never observed. One possible reason is that for our polymer, there is one charged group per 0.4 nm, compared to ≃1 per 0.25 nm[135] for polystyrenesulfonate and poly(1-butyl-3-vinylimidazolium bis(trifluoromethanesulfonyl)imide). This should result in a lower density of condensed counterions and correspondingly weaker counterion-induced attraction. Additionally, the semi-flexible nature of the CMC backbone likely prevents the local collapse of chains into globules.

5.2. Counterion Condensation

The theory of Colby et al. relates the fraction of charged monomers (f) to the specific conductance (Λ) of semi-dilute,[136] salt-free polyelectrolyte solutions as[94]

$$\Lambda = f\left[\lambda_C + \frac{fe^2 c\xi^2 N_A^2 \ln(\xi/D)}{3\pi\eta_s}\right] \quad (8)$$

where λ_C is the limiting specific conductance of the counterion in the solvent, D is the cross-sectional diameter of the chain, taken to be 7 Å in all solvents, N_A is the Avogadro constant, c is the concentration of repeating units per unit volume, and e is the unit of charge. The specific conductances for the TBA ion in various solvents are listed in Table 1.

Equation 8 calculates the conductivity of a polyelectrolyte solution, assuming that free counterions have the same mobility as in a simple salt solution. The contribution of the polymer is estimated as that of a correlation blob (modeled as a cylinder of length ξ and diameter D) multiplied by the number of correlation blobs per chain. Condensed counterions are assumed to not contribute to the solution conductivity.

Figure 9 plots the fraction of monomers bearing a dissociated charge (f) as a function of the polymer concentration for NaCMC and TBACMC. Despite the differences in size and affinity for water between Na^+ and TBA^+, the calculated values of f differ by less than 10%. This reinforces previous findings that while counterion valence has a large influence on polyelectrolyte properties, changing the ion type for a given valence has a much weaker effect.[107,137,138] The slight increase in f at high concentrations is consistent with earlier measurements on NaCMC of various degrees of substitution and also with conductivity and osmotic pressure data of polystyrenesulfonate solutions.[85]

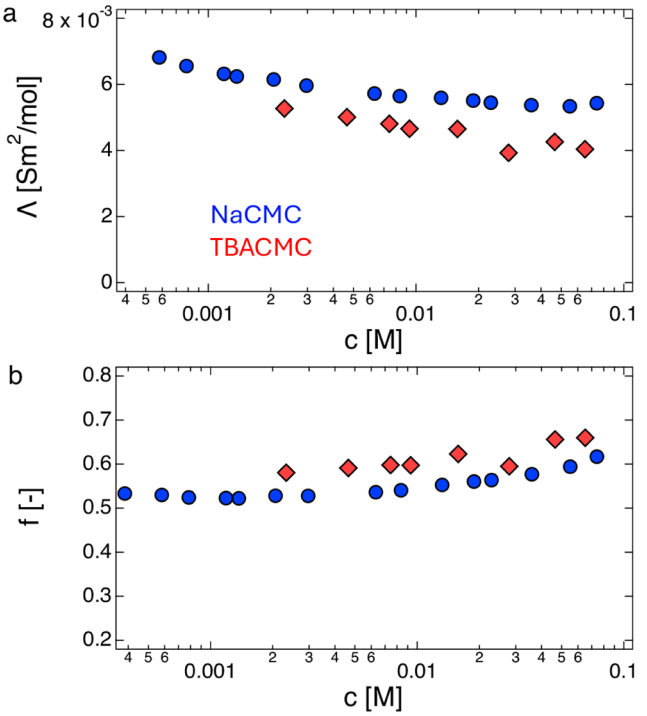

Figure 9. Comparison of conductance (a) and fraction of monomers bearing a dissociated counterion (b) for semidilute solutions of NaCMC and TBACMC as a function of polymer concentration. The values of f are calculated using eq 8 with B = 1 for both salts.

Figure 10a plots the fraction of charged monomers as a function of polymer concentration for TBACMC in different solvents (see Table 1). We use the values of B listed in Table 1 to calculate the correlation length and fix D = 7 Å for all solvents.[95] With these values, eq 8 is used to calculate f for each polymer concentration.

A test for the applicability of the Oosawa-Manning model to semidilute TBACMC solutions is provided in Figure 10b, where the inverse of the fraction of monomers with a dissociated counterion is plotted as a function of l_B. A linear relationship between these two quantities, as expected by eq 1, is observed, but the effective charge density corresponds to approximately one charge per $1.3l_B$, as shown by the dashed black line. These results are in line with earlier studies on the conductivity of NaCMC in water,[80,81,91] which also found charge densities lower than expected by the OM model. Water, NMA, and NMF show $f \simeq 0.65$ despite having different dielectric constants. Equation 1 only expects f to be independent of the Bjerrum length when all counterions are dissociated. The reason for this discrepancy is not clear to us presently.

In an earlier study, we concluded that for NaCMC in water, eq 8 likely underestimates the fraction of dissociated counterions because it assumes that the dissociated counterion mobility is equal to that of the free ion.[80] The actual fraction of free counterions may therefore be somewhat closer to eq 1 than the values shown in Figure 10. The simplifications introduced by the Oosawa-Manning model might also cause an error of order unity in the estimate for the charge fraction.

The red line in Figure 10 is calculated assuming a monomer size of b = 5.15 Å. However, as discussed above, the stretching parameter data suggest that the effective monomer size may be lower in some solvents. The question then arises as to whether

https://doi.org/10.1021/acsapm.6c00522
ACS Appl. Polym. Mater. 2026, 8, 8183−8197

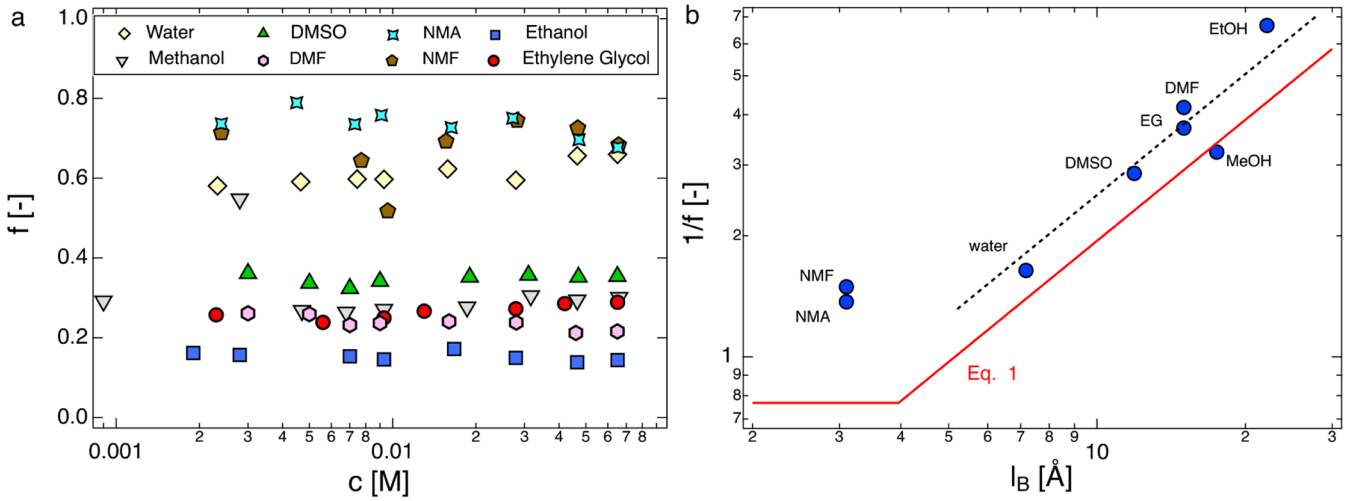

Figure 10. (a) Fraction of monomers with a dissociated counterion (f) as a function of polymer concentration for TBACMC solutions. f is calculated using eq 8. (b) Reciprocal of the fraction of monomers with a dissociated counterion as a function of Bjerrum length (l_B). Values of f are averaged over all concentrations in part a. The red line is eq 1 with n = DS = 1.3 and b = 5.15 Å. Note that $f^{-1} \simeq 0.77$ is predicted in the low l_B limit, corresponding to 1.3 dissociated counterions per monomer. The dashed line, which lies 30% above the red line, corresponds to the best-fit line for $l_B > 5$ Å.

using b = 5.15 Å gives the correct distance between charges. In order to answer this, it would be necessary to know whether folding of the CMC chain occurs on length scales smaller or larger than the distance between charges, but we lack such information.

6. CONCLUSIONS

Our results demonstrate a clear dependence of the effective charge fraction on the solvent's dielectric constant. At fixed polymer concentration, the fraction of dissociated monomers, f, scales approximately with the inverse Bjerrum length, in qualitative agreement with the Oosawa-Manning condensation model. However, differences in f for solvents with similar dielectric constants suggest that continuum electrostatics alone may not fully explain counterion condensation.

The stretching parameter B, extracted from small-angle scattering measurements, was found to be solvent-dependent. High-permittivity solvents such as NMA, NMF, water, and DMSO yield B values close to unity, consistent with semiflexible chains that are fully stretched inside the correlation blobs. This value is consistent with literature results for semiflexible polyelectrolytes, including DNA and several polysaccharides. Lower-permittivity solvents such as methanol, ethanol, and DMF exhibit larger B values, suggesting partial folding within the correlation blob, but the origin of this effect remains unclear. At present, it is not known whether the higher values of the stretching parameter reflect solvent-driven changes in the intrinsic (nonelectrostatic) conformation of the cellulose backbone or if electrostatic stretching plays a role.

The scattering data reveal solvent-dependent coupling between the polymer backbone and counterion concentration fluctuations. In water and methanol, SANS and SAXS peak positions coincide at low concentrations but diverge at higher concentrations, suggesting a decoupling of the counterion and monomer fluctuations. In ethanol, the peak positions measured by the two techniques remaine equal across the entire concentration range. This suggests that decoupling occurs if f is sufficiently high and/or the counterions are sufficiently solvophobic, but more data are needed to confirm this point.

ASSOCIATED CONTENT

Supporting Information

The Supporting Information is available free of charge at https://pubs.acs.org/doi/10.1021/acsapm.6c00522.

(XLSX)

The SANS and SAXS (I vs q) profiles and conductivity data are tabulated in the Supporting Information (PDF)

AUTHOR INFORMATION

Corresponding Author

Carlos G. Lopez − *Materials Science and Engineering Department, The Pennsylvania State University, State College, Pennsylvania 16802, United States;* orcid.org/0000-0001-6160-632X; Email: cvg5719@psu.edu

Authors

Anish Gulati − *Institute of Physical Chemistry, RWTH Aachen University, Aachen 52056, Germany, European Union;* orcid.org/0000-0003-2312-5634

Lingzi Meng − *Materials Science and Engineering Department, The Pennsylvania State University, State College, Pennsylvania 16802, United States*

Can Hou − *Institute of Physical Chemistry, RWTH Aachen University, Aachen 52056, Germany, European Union;* orcid.org/0009-0001-1611-8439

Takaichi Watanabe − *Department of Applied Chemistry, Graduate School of Environmental, Life, Natural Science and Technology, Okayama University, Okayama 700-8530, Japan;* orcid.org/0000-0002-5855-2583

Complete contact information is available at: https://pubs.acs.org/10.1021/acsapm.6c00522

Notes

The authors declare no competing financial interest.

https://doi.org/10.1021/acsapm.6c00522
ACS Appl. Polym. Mater. 2026, 8, 8183−8197

■ ACKNOWLEDGMENTS

We thank the ILL (10.5291/ILL-DATA.9-11-1961) and the SPring-8 synchrotron radiation facility (Hyogo, Japan) for beamtime at BL40B2 (Proposal number: 2024A1203). We thank Noboru Ohta for help with the SAXS experiments. Hannes Luhmann (RWTH) and the students of the Watanabe group at Okayama University (Rene Iwato, Yume Tao, and Hikari Tsunekawa) are thanked for their help running the SAXS measurements. The authors acknowledge funding from the DFG (project: GO 3250/2-1) and the JSPS KAKENHI projects (JP24K01236 and JP20KK0325). We thank Prof. Atsushi Matsumoto (University of Fukui) for help with the scattering experiments and for providing us with *N*-methylformamide. We thank Ralph H. Colby for useful comments on the manuscript. This work is based on a preprint available at https://polyelectrolyte.science.[139]

■ REFERENCES

(1) Dobrynin, A. V.; Rubinstein, M. Theory of polyelectrolytes in solutions and at surfaces. *Prog. Polym. Sci.* **2005**, *30*, 1049−1118.
(2) Sayko, R.; Tian, Y.; Liang, H.; Dobrynin, A. V. Charged polymers: From polyelectrolyte solutions to polyelectrolyte complexes. *Macromolecules* **2021**, *54*, 7183−7192.
(3) Matsumoto, A. Rheology of polyelectrolyte solutions: Current understanding and perspectives. *Nihon Reoroji Gakkaishi* **2022**, *50*, 43−50.
(4) Matsumoto, A. Solution rheology of poly (ionic liquid) s: Current understanding and open questions. *Korea-Aust. Rheol. J.* **2024**, *36*, 319−328.
(5) Traeger, A.; Leiske, M. N. The Whole Is Greater than the Sum of Its Parts−Challenges and Perspectives in Polyelectrolytes. *Biomacromolecules* **2025**, *26*, 5−32.
(6) Vilsinski, B. H.; de Oliveira, A. C.; Souza, P. R.; Martins, A. F. Polysaccharide-based polyelectrolyte multilayers fabricated via layer-by-layer approach: From preparation to applications. *Prog. Org. Coat* **2024**, *196*, 108720.
(7) Sim, B.; Chang, J. J.; Lin, Q.; Wong, J. H. M.; Ow, V.; Leow, Y.; Wong, Y. J.; Boo, Y. J.; Goh, R.; Loh, X. J. Hydrogels based on polyelectrolyte complexes: Underlying principles and biomedical applications. *Biomacromolecules* **2024**, *25*, 7563−7580.
(8) Li, J.; Li, L.; Brink, H.; Allegri, G.; Lindhoud, S. Polyelectrolyte complex-based materials for separations, progress, challenges and opportunities. *Mater. Horiz.* **2025**, *12*, 4998−5030.
(9) Baddam, V.; Tenhu, H. Thermoresponsive polycations. *Polym. Chem.* **2023**, *14*, 3647−3678.
(10) Tagliabue, A.; Mella, M. The Role of Counterion Size in Defining Star-Shaped Polyelectrolytes Thermodynamics, Conformations, and Ion Dynamics. *J. Polym. Sci.* **2025**, *63*, 3005−3022.
(11) Rubinstein, M.; Papoian, G. A. Polyelectrolytes in biology and soft matter. *Soft Matter* **2012**, *8*, 9265−9267.
(12) Mussel, M.; Basser, P. J.; Horkay, F. Ion-induced volume transition in gels and its role in biology. *Gels* **2021**, *7*, 20.
(13) Horkay, F. Polyelectrolyte gels: A unique class of soft materials. *Gels* **2021**, *7*, 102.
(14) Horkay, F.; Basser, P. J.; Geissler, E. Cartilage extracellular matrix polymers: Hierarchical structure, osmotic properties, and function. *Soft Matter* **2024**, *20*, 6033−6043.
(15) Horkay, F.; Basser, P. J. Organization of hyaluronic acid molecules in solutions. *MRS Adv.* **2024**, *9*, 537−542.
(16) Muthukumar, M. *Physics of Charged Macromolecules*; Cambridge University Press, 2023.
(17) Lopez, C. G.; Matsumoto, A.; Shen, A. Q. Dilute polyelectrolyte solutions: Recent progress and open questions. *Soft Matter* **2024**, *20*, 2635−2687.
(18) Beer, M.; Schmidt, M.; Muthukumar, M. The electrostatic expansion of linear polyelectrolytes: Effects of gegenions, co-ions, and hydrophobicity. *Macromolecules* **1997**, *30*, 8375−8385.
(19) Matsumoto, A.; Ukai, R.; Osada, H.; Sugihara, S.; Maeda, Y. Tuning the solution viscosity of ionic-liquid-based polyelectrolytes with solvent dielectric constants via the counterion condensation. *Macromolecules* **2022**, *55*, 10600−10606.
(20) Gulati, A.; Meng, L.; Watanabe, T.; Lopez, C. G. Electrostatically-Driven Collapse of Polyelectrolytes: The Role of the Solvent's Dielectric Constant. *J. Polym. Sci.* **2025**, *63*, 4207−4218.
(21) Chremos, A.; Douglas, J. F. Polyelectrolyte association and solvation. *J. Chem. Phys.* **2018**, *149*, 163305.
(22) Chremos, A.; Douglas, J. F. Communication: When does a branched polymer become a particle? *J. Chem. Phys.* **2015**, *143*, 111104.
(23) Gavrilov, A.; Chertovich, A.; Kramarenko, E. Y. Conformational behavior of a single polyelectrolyte chain with bulky counterions. *Macromolecules* **2016**, *49*, 1103−1110.
(24) Gordievskaya, Y. D.; Gavrilov, A. A.; Kramarenko, E. Y. Effect of counterion excluded volume on the conformational behavior of polyelectrolyte chains. *Soft Matter* **2018**, *14*, 1474−1481.
(25) Kondou, S.; Sakashita, Y.; Morinaga, A.; Katayama, Y.; Dokko, K.; Watanabe, M.; Ueno, K. Concentrated nonaqueous polyelectrolyte solutions: High Na-ion transference number and surface-tethered polyanion layer for sodium-metal batteries. *ACS Appl. Mater. Interfaces* **2023**, *15*, 11741−11755.
(26) Gao, X.; Yamamoto, K.; Hirai, T.; Ohta, N.; Uchiyama, T.; Watanabe, T.; Imai, H.; Sugawara, S.; Shinohara, K.; Uchimoto, Y. Impact of the composition of alcohol/water dispersion on the proton transport and morphology of cast perfluorinated sulfonic acid ionomer thin films. *ACS Omega* **2021**, *6*, 14130−14137.
(27) Qiu, Y.; Zhao, X.; Li, H.; Liu, S.; Yu, W. Microstructures and Rheological Properties of Short-Side-Chain Perfluorosulfonic Acid in Water/2-Propanol. *Polymers* **2024**, *16*, 1863.
(28) Wang, S.; Song, J.; Zhao, W.; Guan, P.; Li, M.; Zhang, M.; Zou, Y.; Liu, J.; Chen, G.; Ren, H.; et al. Nanostructures and multi-scale aggregation of high ion exchange capacity short-side-chain perfluorosulfonic acid dispersion. *J. Colloid Interface Sci.* **2024**, *672*, 805−813.
(29) Shin, J.; Shin, H.; Lee, S.-H.; Jang, J. D.; Kim, H. J. Influence of Solvent Dielectric Constant on the Complex Coacervation Phase Behavior of Polymerized Ionic Liquids. *ACS Macro Lett.* **2024**, *13*, 1678−1685.
(30) Novy, M.; Duchesne, D.; Dahlke, G.; Chen, L. P.; Moore, R. B. Effect of Ionomer−Solvent Interactions in PFSA Dispersions: Dispersion Morphology. *Macromolecules* **2025**, *58*, 8854−8865.
(31) Oosawa, F. A simple theory of thermodynamic properties of polyelectrolyte solutions. *J. Polym. Sci.* **1957**, *23*, 421−430.
(32) Manning, G. S. Limiting laws and counterion condensation in polyelectrolyte solutions I. Colligative properties. *J. Chem. Phys.* **1969**, *51*, 924−933.
(33) Manning, G. S. The molecular theory of polyelectrolyte solutions with applications to the electrostatic properties of polynucleotides. *Q. Rev. Biophys.* **1978**, *11*, 179−246.
(34) Chen, G.; Perazzo, A.; Stone, H. A. Electrostatics, conformation, and rheology of unentangled semidilute polyelectrolyte solutions. *J. Rheol.* **2021**, *65*, 507−526.
(35) Marioni, N.; Rajesh, A.; Zhang, Z.; Freeman, B. D.; Ganesan, V. What is the influence of ion aggregation and counterion condensation on salt transport in ion exchange membranes? *J. Membr. Sci.* **2024**, *701*, 122713.
(36) Wandrey, C. Concentration regimes in polyelectrolyte solutions. *Langmuir* **1999**, *15*, 4069−4075.
(37) Wandrey, C.; Hunkeler, D.; Wendler, U.; Jaeger, W. Counterion activity of highly charged strong polyelectrolytes. *Macromolecules* **2000**, *33*, 7136−7143.
(38) Liao, Q.; Dobrynin, A. V.; Rubinstein, M. Molecular dynamics simulations of polyelectrolyte solutions: Osmotic coefficient and counterion condensation. *Macromolecules* **2003**, *36*, 3399−3410.
(39) Nyquist, R. M.; Ha, B.-Y.; Liu, A. J. Counterion condensation in solutions of rigid polyelectrolytes. *Macromolecules* **1999**, *32*, 3481−3487.

(40) Muthukumar, M. Theory of counter-ion condensation on flexible polyelectrolytes: Adsorption mechanism. *J. Chem. Phys.* **2004**, *120*, 9343−9350.
(41) Kundagrami, A.; Muthukumar, M. Theory of competitive counterion adsorption on flexible polyelectrolytes: Divalent salts. *J. Chem. Phys.* **2008**, *128*, 244901.
(42) Kumar, R.; Kundagrami, A.; Muthukumar, M. Counterion adsorption on flexible polyelectrolytes: Comparison of theories. *Macromolecules* **2009**, *42*, 1370−1379.
(43) This is in contrast to the scaling model, which expects the conformation of a polyelectrolyte chain to be independent of the effective charge fraction if the Bjerrum length is smaller than the intrinsic Kuhn segment of the polymer.
(44) Dou, S.; Colby, R. H. Charge density effects in salt-free polyelectrolyte solution rheology. *J. Polym. Sci., Part B: Polym. Phys.* **2006**, *44*, 2001−2013.
(45) Kowblansky, M.; Zema, P. Interactions of sodium ions with the sodium salts of poly (acrylic acid/acrylamide) copolymers of varying charge density. *Macromolecules* **1981**, *14*, 166−170.
(46) Dobrynin, A. V.; Colby, R. H.; Rubinstein, M. Scaling theory of polyelectrolyte solutions. *Macromolecules* **1995**, *28*, 1859−1871.
(47) Jousset, S.; Bellissent, H.; Galin, J. C. Polyelectrolytes of high charge density in organic solvents. Synthesis and viscosimetric behavior. *Macromolecules* **1998**, *31*, 4520−4530.
(48) Lee, M.; Perry, S. L.; Hayward, R. C. Complex coacervation of polymerized ionic liquids in non-aqueous solvents. *ACS Polym. Au* **2021**, *1*, 100−106.
(49) Hou, C.; Watanabe, T.; Lopez, C. G.; Richtering, W. Structure and rheology of carboxymethylcellulose in polar solvent mixtures. *Carbohydr. Polym.* **2025**, *347*, 122287.
(50) Marcilla, R.; Alberto Blazquez, J.; Rodriguez, J.; Pomposo, J. A.; Mecerreyes, D. Tuning the solubility of polymerized ionic liquids by simple anion-exchange reactions. *J. Polym. Sci., Part A: Polym. Chem.* **2004**, *42*, 208−212.
(51) Ono, T.; Sugimoto, T.; Shinkai, S.; Sada, K. Lipophilic polyelectrolyte gels as super-absorbent polymers for nonpolar organic solvents. *Nat. Mater.* **2007**, *6*, 429−433.
(52) Ono, T.; Sugimoto, T.; Shinkai, S.; Sada, K. Molecular design of superabsorbent polymers for organic solvents by crosslinked lipophilic polyelectrolytes. *Adv. Funct. Mater.* **2008**, *18*, 3936−3940.
(53) Ono, T.; Ohta, M.; Iseda, K.; Sada, K. Counter anion dependent swelling behaviour of poly (octadecyl acrylate)-based lipophilic polyelectrolyte gels as superabsorbent polymers for organic solvents. *Soft Matter* **2012**, *8*, 3700−3704.
(54) Ono, T.; Ohta, M.; Sada, K. Ionic polymers act as polyelectrolytes in nonpolar media. *ACS Macro Lett.* **2012**, *1*, 1270−1273.
(55) Chen, J.; Wang, S.; Peng, J.; Li, J.; Zhai, M. New lipophilic polyelectrolyte gels containing quaternary ammonium salt with superabsorbent capacity for organic solvents. *ACS Appl. Mater. Interfaces* **2014**, *6*, 14894−14902.
(56) Gulati, A.; Lopez, C. G. Viscosity of polyelectrolytes: Influence of counterion and solvent type. *ACS Macro Lett.* **2024**, *13*, 1079−1083.
(57) Hou, C.; Richtering, W.; Watanabe, T.; Leonhard, K.; Papusha, M.; Lopez, C. G. Solutions of Carboxymethylcellulose with Organic Counterions (I): The Influence of Counterion Properties on the Polymer Structure and Solubility. *Macromolecules* **2025**, *58*, 7489−7499.
(58) Feddersen, R. L.; Thorp, S. N. *Industrial Gums*; Elsevier, 1993; pp. 537−578.
(59) Stigsson, V.; Wilson, D. I.; Germgärrd, U. Production variance in purified carboxymethyl cellulose (CMC) manufacture. *Dev. Chem. Eng. Miner. Process* **2004**, *12*, 217−231.
(60) Stigsson, V.; Kloow, G.; Germgård, U. An historic overview of carboxymethyl cellulose (CMC) production on an industrial scale. *PaperAsia* **2001**, 17.
(61) Barba, C.; Montané, D.; Rinaudo, M.; Farriol, X. Synthesis and characterization of carboxymethylcelluloses (CMC) from non-wood fibers I. Accessibility of cellulose fibers and CMC synthesis. *Cellulose* **2002**, *9*, 319−326.
(62) Lopez, C. G.; Colby, R. H.; Cabral, J. T. Electrostatic and hydrophobic interactions in NaCMC aqueous solutions: Effect of degree of substitution. *Macromolecules* **2018**, *51*, 3165−3175.
(63) Lopez, C. G.; Richtering, W. Oscillatory rheology of carboxymethyl cellulose gels: Influence of concentration and pH. *Carbohydr. Polym.* **2021**, *267*, 118117.
(64) Rahman, M. S.; Hasan, M. S.; Nitai, A. S.; Nam, S.; Karmakar, A. K.; Ahsan, M. S.; Shiddiky, M. J.; Ahmed, M. B. Recent developments of carboxymethyl cellulose. *Polymers* **2021**, *13*, 1345.
(65) Ramakrishnan, R.; Kim, J. T.; Roy, S.; Jayakumar, A. Recent advances in carboxymethyl cellulose-based active and intelligent packaging materials: A comprehensive review. *Int. J. Biol. Macromol.* **2024**, *259*, 129194.
(66) Zennifer, A.; Senthilvelan, P.; Sethuraman, S.; Sundaramurthi, D. Key advances of carboxymethyl cellulose in tissue engineering & 3D bioprinting applications. *Carbohydr. Polym.* **2021**, *256*, 117561.
(67) Rinaudo, M.; Mazet, J.; Milas, M. Propriétés thermodynamiques des polyanions à Densité de charge variable. *C. R. Acad. Sci.* **1973**, 1401−1404.
(68) Rinaudo, M.; Loiseleu, B.; Milas, M. Determination Of Dissociation Constant Of Polyacids By Potentiometry. *C. R. Acad. Sci., Ser. C* **1971**, *273*, 1148.
(69) Rinaudo, M.; Milas, M. Interaction of monovalent and divalent counterions with some carboxylic polysaccharides. *J. Polym. Sci. Polym. Chem. Ed.* **1974**, *12*, 2073−2081.
(70) Rinaudo, M.; Mils, M. Polyelectroyte behavior of a bacterial polysaccharide from Xanthomonas campestris: Comparison with carboxymethylcellulose. *Biopolymers* **1978**, *17*, 2663−2678.
(71) Rinaudo, M. Polyelektrolyteigenschaften von carboxymethylcellulose in wäbriger lösung. Einfluß der ladungsdichte. *Faserforsch. Textiltech* **1973**, 21−28.
(72) Rinaudo, M.; Milas, M. *Polyelectrolytes and their Applications*; Springer, 1975; pp. 31−49.
(73) Nagasawa, M.; Kagawa, I. Colligative properties of polyelectrolyte solutions. IV. Activity coefficient of sodium ion. *J. Polym. Sci.* **1957**, *25*, 61−76.
(74) Rinaudo, M.; Pierre, C. Volume spécifique partiel des polyélectrolytes. *C. R. Acad. Sci.* **1969**, 1280.
(75) Rinaudo, M.; Milas, M. Propriétés électrochimiques des polyélectrolytes à Densité de charge élevée. *J. Chim. Phys.* **1969**, *66*, 1489−1496.
(76) Zana, R.; Tondre, C.; Rinaudo, M.; Milas, M. Étude ultrasonore de la fixation sur site des ions alcalins sur des carboxymethylcelluloses de Densité de charge variable. *J. Chim. Phys.* **1971**, *68*, 1258−1266.
(77) Tondre, C.; Zana, R. Ultrasonic absorption as a probe for the study of site binding of counterions in polyelectrolyte solutions. *J. Phys. Chem.* **1971**, *75*, 3367−3372.
(78) Tondre, C.; Zana, R. Apparent molal volumes of polyelectrolytes in aqueous solutions. *J. Phys. Chem.* **1972**, *76*, 3451−3459.
(79) Zana, R. Studies of Aqueous Solutions of Polyelectrolytes by Means of Ultrasonic Methods. *J. Macromol. Sci., Rev. Macromol. Chem.* **1975**, *12*, 165−189.
(80) Abbasi GharehTapeh, E.; Watanabe, T.; Horkay, F.; Hou, C.; Lopez, C. G.; Hohenschutz, M. Counterion condensation, ion pairing and scattering properties of carboxymethyl cellulose with mono- and di-valent ions. *Cellulose, submitted* **2026**, 1−20.
(81) Truzzolillo, D.; Bordi, F.; Cametti, C.; Sennato, S. Counterion condensation of differently flexible polyelectrolytes in aqueous solutions in the dilute and semidilute regime. *Phys. Rev. E* **2009**, *79*, 011804.
(82) Truzzolillo, D.; Cametti, C.; Sennato, S. Dielectric properties of differently flexible polyions: A scaling approach. *Phys. Chem. Chem. Phys.* **2009**, *11*, 1780−1786.
(83) Gulati, A.; Douglas, J. F.; Matsarskaia, O.; Lopez, C. G. Influence of counterion type on the scattering of a semiflexible polyelectrolyte. *Soft Matter* **2024**, *20*, 8610−8620.

https://doi.org/10.1021/acsapm.6c00522
ACS Appl. Polym. Mater. 2026, 8, 8183−8197

(84) Combet, J.; Isel, F.; Rawiso, M.; Boué, F. Scattering functions of flexible polyelectrolytes in the presence of mixed valence counterions: Condensation and scaling. *Macromolecules* **2005**, *38*, 7456−7469.
(85) Bordi, F.; Cametti, C.; Colby, R. Dielectric spectroscopy and conductivity of polyelectrolyte solutions. *J. Phys.: Condens. Matter.* **2004**, *16*, R1423.
(86) Nandi, P.; Das, B. Effects of concentration, relative permittivity, and temperature on the solution behavior of sodium carboxymethylcellulose as probed by electrical conductivity. *J. Phys. Chem. B* **2005**, *109*, 3238−3242.
(87) Nandi, P. *Solution Properties of Sodium Carboxymethylcellulose in Acetonitrile -Water Mixed Solvent Media*; Ph.D. thesis, 2009.
(88) Nandi, P.; Das, B. Electrical conductances of sodium carboxymethylcellulose in acetonitrile (1)+ water (2) mixed solvent media in the presence of sodium chloride at 308.15 K. *J. Chem. Eng. Data* **2011**, *56*, 2870−2876.
(89) Chatterjee, A.; Das, B.; Das, C. Polyion−counterion interaction behavior for sodium carboxymethylcellulose in methanol−water mixed solvent media. *Carbohydr. Polym.* **2012**, *87*, 1144−1152.
(90) Sharma, R.; Das, C.; Dahal, S.; Das, B. Polyion−counterion interactions in sodium carboxymethylcellulose−ethylene glycol−water ternary solutions. *Carbohydr. Polym.* **2013**, *92*, 1546−1554.
(91) Ray, D.; De, R.; Das, B. Thermodynamic, transport and frictional properties in semidilute aqueous sodium carboxymethylcellulose solution. *J. Chem. Thermodyn* **2016**, *101*, 227−235.
(92) Das, B.; Chatterjee, A. Salt-induced counterion condensation and related phenomena in sodium carboxymethylcellulose−sodium halide−methanol−water quaternary systems. *Soft Matter* **2015**, *11*, 4133−4140.
(93) Das, C.; Sharma, B.; Das, B. Studies on counterion-condensation in sodium carboxymethylcellulose-2-butoxyethanol-water ternaries using electrical conductivity. *J. Mol. Liq.* **2016**, *219*, 104−110.
(94) Colby, R. H.; Boris, D. C.; Krause, W. E.; Tan, J. S. Polyelectrolyte conductivity. *J. Polym. Sci., Part B: Polym. Phys.* **1997**, *35*, 2951−2960.
(95) Lopez, C. G.; Rogers, S. E.; Colby, R. H.; Graham, P.; Cabral, J. T. Structure of sodium carboxymethyl cellulose aqueous solutions: A SANS and rheology study. *J. Polym. Sci., Part B: Polym. Phys.* **2015**, *53*, 492−501.
(96) Sharratt, W. N.; O'Connell, R.; Rogers, S. E.; Lopez, C. G.; Cabral, J. T. Conformation and phase behavior of sodium carboxymethyl cellulose in the presence of mono-and divalent salts. *Macromolecules* **2020**, *53*, 1451−1463.
(97) De Gennes, P.-G.; Pincus, P.; Velasco, R.; Brochard, F. Remarks on polyelectrolyte conformation. *J. Phys.* **1976**, *37*, 1461−1473.
(98) Lopez, C. G.; Colby, R. H.; Graham, P.; Cabral, J. T. Viscosity and scaling of semiflexible polyelectrolyte NaCMC in aqueous salt solutions. *Macromolecules* **2017**, *50*, 332−338.
(99) Jimenez, L. N.; Martinez Narvaez, C. D.; Sharma, V. Solvent Properties Influence the Rheology and Pinching Dynamics of Polyelectrolyte Solutions: Thickening the Pot with Glycerol and Cellulose Gum. *Macromolecules* **2022**, *55* (18), 8117−8132.
(100) Wagner, P.; Różańska, S.; Warmbier, E.; Frankiewicz, A.; Różański, J. Rheological properties of sodium carboxymethylcellulose solutions in dihydroxy alcohol/water mixtures. *Materials* **2023**, *16*, 418.
(101) Komorowska, P.; Różańska, S.; Różański, J. Effect of the degree of substitution on the rheology of sodium carboxymethylcellulose solutions in propylene glycol/water mixtures. *Cellulose* **2017**, *24*, 4151−4162.
(102) Różańska, S.; Verbeke, K.; Różański, J.; Clasen, C.; Wagner, P. Capillary breakup extensional rheometry of sodium carboxymethylcellulose solutions in water and propylene glycol/water mixtures. *J. Polym. Sci., Part B: Polym. Phys.* **2019**, *57*, 1537−1547.
(103) Kassapidou, K.; Jesse, W.; Kuil, M.; Lapp, A.; Egelhaaf, S.; Van der Maarel, J. Structure and charge distribution in DNA and poly (styrenesulfonate) aqueous solutions. *Macromolecules* **1997**, *30*, 2671−2684.
(104) Van der Maarel, J.; Groot, L.; Hollander, J.; Jesse, W.; Kuil, M.; Leyte, J.; Leyte-Zuiderweg, L.; Mandel, M.; Cotton, J. On the charge distribution in aqueous poly (styrenesulfonic acid) solutions. A small-angle neutron scattering study. *Macromolecules* **1993**, *26*, 7295−7299.
(105) *Neutron scattering lengths and cross sections*; https://www.ncnr.nist.gov/resources/n-lengths/.
(106) Marcus, Y. Tetraalkylammonium ions in aqueous and non-aqueous solutions. *J. Solution Chem.* **2008**, *37*, 1071−1098.
(107) Lopez, C. G.; Richtering, W. Influence of divalent counterions on the solution rheology and supramolecular aggregation of carboxymethyl cellulose. *Cellulose* **2019**, *26*, 1517−1534.
(108) Lopez, C. G. Entanglement of semiflexible polyelectrolytes: Crossover concentrations and entanglement density of sodium carboxymethyl cellulose. *J. Rheol.* **2020**, *64*, 191−204.
(109) Gulati, A. *Polyelectrolyte Conformation and Rheology in solutions*; Ph.D. thesis, RWTH Aachen, 2024.
(110) Sehgal, A.; Seery, T. A. Polyelectrolyte self-diffusion: Fluorescence recovery after photobleaching of sodium poly (styrenesulfonate) in N-methylformamide. *Macromolecules* **2003**, *36*, 10056−10062.
(111) Dou, S. *Synthesis and characterization of ion-containing polymers*; Ph.D. thesis, 2007.
(112) Dou, S.; Colby, R. H. Solution rheology of a strongly charged polyelectrolyte in good solvent. *Macromolecules* **2008**, *41*, 6505−6510.
(113) Cohen, J.; Priel, Z.; Rabin, Y. Viscosity of dilute polyelectrolyte solutions. *J. Chem. Phys.* **1988**, *88*, 7111−7116.
(114) An exception to this are the H^+ and OH^- ions, which have higher mobilities and as a result conduct more than alkali metal or halide ions.
(115) Vink, H. Electrolytic conductivity of polyelectrolyte solutions. *Makromol. Chem.* **1982**, *183*, 2273−2283.
(116) Viscosity data for TBAPSS in this same solvent also suggest a high residual salt content. We do not have a way to explain why this is the case at present because the presence of any ionic component is expected to show up in the solution conductivity.
(117) Smolyakov, G.; Catala, J.-M.; Kutsevol, N.; Rawiso, M. Influence of the Nature of Counterions and Solvent on the Structure of PSS Solutions. In*Modern Problems of Molecular Physics: Selected Reviews from the 7th International Conference Physics of Liquid Matter*: Modern Problems: Kyiv, Ukraine, May 27−31, 2016. 2017; pp 133−147.
(118) Spiteri, M. *Conformation and arrangement of polyelectrolytes in semi-diluted solution. A study by small angle neutron scattering; Conformation et arrangement des polyelectrolytes en solution semi-diluee. Etude par diffusion des neutrons aux petits angles*; Semantic Scholar 1997.
(119) Nishida, K.; Kaji, K.; Kanaya, T.; Shibano, T. Added salt effect on the intermolecular correlation in flexible polyelectrolyte solutions: Small-angle scattering study. *Macromolecules* **2002**, *35*, 4084−4089.
(120) We assume f = 0.5 for CMC and f = 0.3 for NaPSS following refs. [80,85]
(121) Salamon, K.; Aumiler, D.; Pabst, G.; Vuletic, T. Probing the mesh formed by the semirigid polyelectrolytes. *Macromolecules* **2013**, *46*, 1107−1118.
(122) Nishida, K.; Kaji, K.; Kanaya, T. High concentration crossovers of polyelectrolyte solutions. *J. Chem. Phys.* **2001**, *114*, 8671−8677.
(123) Douglas, J. F.; Horkay, F.; Zhang, Y. Influence of counterion valency on the scattering properties of highly charged polyelectrolyte solutions revisited. *J. Chem. Phys.* **2025**, *163*, 154905.
(124) Horkay, F.; Basser, P. J.; Hecht, A.-M.; Geissler, E. Chondroitin sulfate in solution: Effects of mono-and divalent salts. *Macromolecules* **2012**, *45*, 2882−2890.
(125) Josef, E.; Bianco-Peled, H. Conformation of a natural polyelectrolyte in semidilute solutions with no added salt. *Soft Matter* **2012**, *8*, 9156−9165.

(126) Wang, L.; Bloomfield, V. A. Small-angle x-ray scattering of semidilute rodlike DNA solutions: Polyelectrolyte behavior. *Macromolecules* **1991**, *24*, 5791−5795.
(127) Borsali, R.; Nguyen, H.; Pecora, R. Small-angle neutron scattering and dynamic light scattering from a polyelectrolyte solution: DNA. *Macromolecules* **1998**, *31*, 1548−1555.
(128) Borsali, R.; Rinaudo, M.; Noirez, L. Light scattering and small-angle neutron scattering from polyelectrolyte solutions: The succinoglycan. *Macromolecules* **1995**, *28*, 1085−1088.
(129) Koyama, R. Small-angle scattering of polyelectrolyte solutions. *Macromolecules* **1986**, *19*, 178−182.
(130) Nishida, K.; Kaji, K.; Kanaya, T. Charge density dependence of correlation length due to electrostatic repulsion in polyelectrolyte solutions. *Macromolecules* **1995**, *28*, 2472−2475.
(131) Dawson, L. R.; Wilhoit, E. D.; Holmes, R. R.; Sears, P. G. Solvents Having High Dielectric Constants. V. Limiting Ionic Equivalent Conductances in N-Methylacetamide at 40°. *J. Am. Chem. Soc.* **1957**, *79*, 3004−3006.
(132) Williams, W. D.; Ellard, J. A.; Dawson, L. R. Solvents having high dielectric constants. VI. Diffusion in N-methylacetamide1, 2. *J. Am. Chem. Soc.* **1957**, *79*, 4652−4654.
(133) Tsierkezos, N. G.; Philippopoulos, A. I. Studies of ion solvation and ion association of n-tetrabutylammonium hexafluorophosphate and n-tetrabutylammonium tetraphenylborate in various solvents. *Fluid Phase Equilib.* **2009**, *277*, 20−28.
(134) Lopez, C. G.; Matsumoto, A.; Gulati, A.; Hou, C.; Mizutani, Y.; Osada, H.; Tao, Y.; Fujii, K.; Richtering, W.; Watanabe, T. Structure of poly (ionic liquid) s in solutions: A small angle scattering study. *ChemRxiv* **2023**.
(135) This assumes b = 0.25 nm for NaPSS. A lower value of 0.17 nm for the effective monomer size was reported by van der Maarel and co-workers which would imply a higher charge density.
(136) Note that f is the fraction of monomers with a dissociated charge, not the fraction of dissociated counterions.
(137) Dubois, E.; Boué, F. Conformation of poly (styrenesulfonate) polyions in the presence of multivalent ions: Small-angle neutron scattering experiments. *Macromolecules* **2001**, *34*, 3684−3697.
(138) Zhang, Y.; Douglas, J. F.; Ermi, B. D.; Amis, E. J. Influence of counterion valency on the scattering properties of highly charged polyelectrolyte solutions. *J. Chem. Phys.* **2001**, *114*, 3299−3313.
(139) Gulati, A.; Meng, L.; Hou, C.; Watanabe, T.; Lopez, C. Solution structure and counterion condensation of carboxymethyl cellulose in organic solvents. 2026.

https://doi.org/10.1021/acsapm.6c00522
ACS Appl. Polym. Mater. 2026, 8, 8183−8197